ACS chemical biology

Letters

pubs.acs.org/acschemicalbiology

Live Intracellular Super-Resolution Imaging Using Site-Specific Stains

Lina Carlini and Suliana Manley*

Laboratory of Experimental Biophysics, École Polytechnique Fédérale de Lausanne, Lausanne, Switzerland

Supporting Information

ABSTRACT: Point localization super-resolution imaging (SR) requires dyes that can cycle between fluorescent and dark states, in order for their molecular positions to be localized and create a reconstructed image. Dyes should also densely decorate biological features of interest to fully reveal structures being imaged. We tested site-specific dyes in several live-cell compatible imaging media and evaluated their performance *in situ*. We identify a number of new dyes and imaging medium-dye combinations for live staining, that densely highlight intracellular structures with excellent photophysical performance for SR.

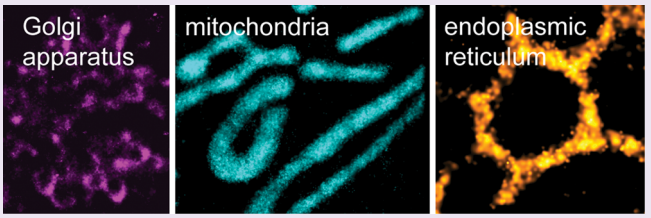

Fluorescence microscopy of living cells reveals dynamic processes of specific protein-enriched structures and organelles. This was extended to the nanoscale by several optical nanoscopy methods, including imaging with photoswitching and localization super-resolution microscopy (SR), as in photoactivated localization microscopy (PALM)[1] or stochastic optical reconstruction microscopy (STORM).[2,3] A common feature of live-cell SR is overexpression of protein fusions, either to fluorescent proteins or chemical targets such as the SNAP-tag or Halo-tag for synthetic dyes. The achievable resolution depends on the density and brightness of fluorophores, since the density of dyes must be high enough to sample the structure at the desired resolution and the localization precision depends to first order on the brightness as the inverse square root of the number of photons. Thus, expression levels should be high, and synthetic dyes are preferred to fluorescent proteins. Among the drawbacks of this approach, few chemically targeted cell-permeable dyes exist for intracellular imaging.[2−4] Furthermore, multicolor imaging is needed to provide cellular context[5] but can be difficult to achieve consistently with transfection.

A complementary labeling strategy for live intracellular SR uses site-specific stains, which do not require transfection, to label cells with high efficiency. These dyes are easily targeted and cell permeable. This strategy was recently demonstrated in SR imaging of DNA,[6] the plasma membrane, and several intracellular compartments.[7] However, this method has not been optimized for live-cell compatibility. Moreover, many other intracellular targets and dyes exist, which have not been examined for live-cell SR. To expand this complementary labeling strategy and enable multicolor imaging, additional site-specific stains should be identified. Lastly, a relationship between chemical structures and intracellular environments that support photoswitching has not been established; this would allow for intelligent design of further site-specific dyes for SR.

In this study, we investigate photoswitching under imaging media and light exposure conditions chosen to reduce toxicity and expand the palette of dyes and target organelles that can be used for intracellular SR imaging. This also allows us to examine correlations between chemical structure and intracellular photoswitching of these high-density labels for live-cell SR.

Early developments in SR with standard organic dyes relied on oxygen depletion and the use of millimolar concentrations of toxic reducing agents, such as betamercaptoethanol, to induce photoswitching.[8−10] Oxygen depletion poses a major constraint on live-cell experiments, since it diminishes ATP production.[11] This is especially a setback when studying mitochondria structure and dynamics,[12] but also disrupts other cellular functions. Another cytotoxic effect that arises from imaging with an oxygen depletion or scavenging system is buffer acidification.[13] Accordingly, this method was exclusively used with fixed cells until the need for an oxygen depletion system was eliminated[14] and lower concentrations of toxic, and even nontoxic,[14,15] reducing agents were used. Conveniently, the endogenous environment of a cell has also proven to be efficient in making a limited number of cell permeable dyes photoswitch in a few cellular compartments.[2,4,16−18] Despite such developments, it is still common to introduce exogenous reducing agents and oxygen depletion systems in performing live cell experiments[3,6,7] for SR imaging of additional targets and dyes.

We screened site-specific stains whose photoswitching in living cells was not previously reported, using several low-toxicity imaging media. These were Leibovitz CO_2-independent medium,[4] and the supplemented buffers Leibovitz with ascorbic acid (AA) as a reducing agent,[19] and Leibovitz with AA and the glucose−oxidase/catalase oxygen removal system (Glox).[6] We

Received: June 26, 2013
Accepted: September 30, 2013

dx.doi.org/10.1021/cb400467x | *ACS Chem. Biol.* XXXX, XXX, XXX−XXX

Table 1. Site-Specific Stains and the Imaging Medium Conditions under Which SR Imaging Was Achieved[a]

site targeted	dye	necessary 405 illumination	Leib	100 μM AA	Glox + 100 μM AA	description of poor (−) conditions	comments
mitochondrial inner membrane/ matrix	rhodamine 123	no	−	+	--	dye aggregation with Glox, unsuitable without AA (see Case 2 in caption).	cationic dye, stains matrix due to negative potential
	JC-9	no	−	−	+	unsuitable without Glox (see Case 2 in caption)	carbocyanine dye, same properties as JC1. Aggregated red form in polarized mitochondria[34]
	TMRE	no	+	+	+		rhodamine derivative, labels inner and outer sides of inner membrane based on potential[35]
Golgi	dye D	yes	+	--	--	dye aggregation with AA or Glox	Benzophenoxazine dye, derivative of Nile Red observed to accumulate in golgi,[36] targeting mechanism not identified
ER/mitochondrial membranes	Nile red	no	+	+	--	dye aggregation and mislocalization with Glox	lipophilic dye
lysosomal interior	LysoTracker Green	yes	−	−	+	unsuitable without Glox (see case 1 in caption)	redox-active organelle, H+ ATPases on membranes, contains hydrolytic enzymes[37]

[a]Good conditions for photoswitching and imaging are denoted by '+' and poor conditions are denoted by '−'. Poor conditions are described by case 1 or case 2. Case 1: once dye bleaches, no single molecule photoswitching begins. Case 2: the number of localizations over time decreases rapidly, preventing a high enough density of localizations to reconstruct an image, see SI Figure 4 for details. In cases where the buffer conditions perturbed the dye a '--' is marked, see SI Figure 2. Leibovitz denoted 'Leib'.

reduced the toxicity of the Glox mixture by using lower levels of Glox: concentrations of catalase and glucose oxidase were approximately 4 and 16 times more dilute than previously reported with such dyes.[7] Accordingly, we measured no drop in pH over the course of the experiments, which lasted up to 20 min. A more in depth look at the toxicity of these dyes and buffers is presented in Supporting Information (SI), Table 1 and Figure 1. Our results, summarized in Table 1, show that numerous new site-specific dyes in different intracellular compartments can be made to photoswitch under one or more of these conditions. Conveniently, we noticed that some of the dyes photoswitch well in living cells imaged in pure Leibovitz buffer; this medium is the least toxic of the three, since it is designed to support cell growth in a CO_2-free atmosphere,[20] and thus represents a preferred imaging environment. To our knowledge, this is the first instance of site-specific dyes being used for SR (PALM/STORM) imaging in the absence of an oxygen scavenging system and without any exogenous reducing agent. We also found that several site-specific stains recently used for live-cell SR in the presence of Glox can perform well in Leibovitz without Glox (SI Table 2). Intriguingly, we noted that the addition of AA or Glox+AA sometimes appeared to be perturbative, not because it disrupted photoswitching but because it resulted in a nonuniform or aggregated staining pattern on the structure of interest (see Table 1 and SI Figure 2 for details); we deem such conditions unsuitable for live-cell imaging. This effect was not consistently observed upon addition of Glox+AA for any specific organelle (Table 1 and SI Table 3); therefore, it is likely due to dye−medium interactions rather than cell perturbations. Several dyes tested entirely failed to produce SR images in any of the tested media (SI Table 3, SI Figures 2−3 for representative wide field images and SI Figure 4 for a quantitative description of these poor photoswitching conditions). We note that although the imaging media clearly has an impact on dye photoswitching, it is always an indirect effect, since the primary determinant is the local internal cellular environment.

Another unfavorable condition for live-cell SR imaging as regards cell health is the use of near UV illumination. Since it is commonly reported to be necessary for recovery from the dark state,[3,7,16,21] irradiation with 405 nm light is often used in photoswitching of synthetic dyes. Conceivably, this illumination could cause less photodamage that that of the imaging laser, which is typically used at higher intensities.[21,22] Still, 405 nm illumination is commonly increased over the course of acquisition to maintain the number of localizations and can significantly induce phototoxicity,[21] photosensitize dyes, and cause cellular damage.[23] Several of the dyes we tested did not require 405 nm illumination to photoswitch and adding 405 nm illumination did not improve image quality (SI Figure 5). We also observed that several site-specific dyes previously reported to perform well with 405 nm illumination (SI Table 2), also did so without. Similarly, the high intensity laser illumination required to achieve single-molecule photoswitching[10] in SR techniques can cause cellular damage. Importantly, we noted that many of the site-specific dyes tested could photoswitch with illumination powers down to 10-fold lower than previously used[7] (SI Figure 6).

Sites targeted by the dyes we screened include the mitochondrial inner membrane/matrix, lipids in the endoplasmic reticulum, the lysosomal interior, and the Golgi apparatus, an organelle never before imaged using live SR techniques. Targeting mechanisms vary with each dye (Table 1). Once suitable imaging conditions were identified, we used these dyes to create live cell SR images of organelles (Figure 1a−e and SI Figures 7−8), which showed improvement over diffraction-limited images (SI Figures 7−8). Note the dense labeling of mitochondria with JC9 (Figure 1a), Rhodamine 123 (Figure 1b), and TMRE (Figure 1c). Due to the high laser intensities, long acquisition times, and toxic imaging media commonly used in live-cell SR, images of mitochondria commonly capture their rounded phenotype. Thus, of particular note here are the elongated morphologies of mitochondria, suggestive of the live-cell compatibility of this method. Additionally, the areas of lower labeling density with TMRE (Figure 1c) are of interest since they allow us to infer the presence of the cristae; such features are not visible in the corresponding diffraction limited image (SI Figure 8). Curiously, however, the cristae are not discernible in SR images from other dyes that label the mitochondrial inner membrane (Figure 1a−b). One possible reason for this lack of resolved substructure could be due to the dyes' photoswitching performance under the tested conditions. For instance, several overlapping molecules could remain in a

dx.doi.org/10.1021/cb400467x | ACS Chem. Biol. XXXX, XXX, XXX−XXX

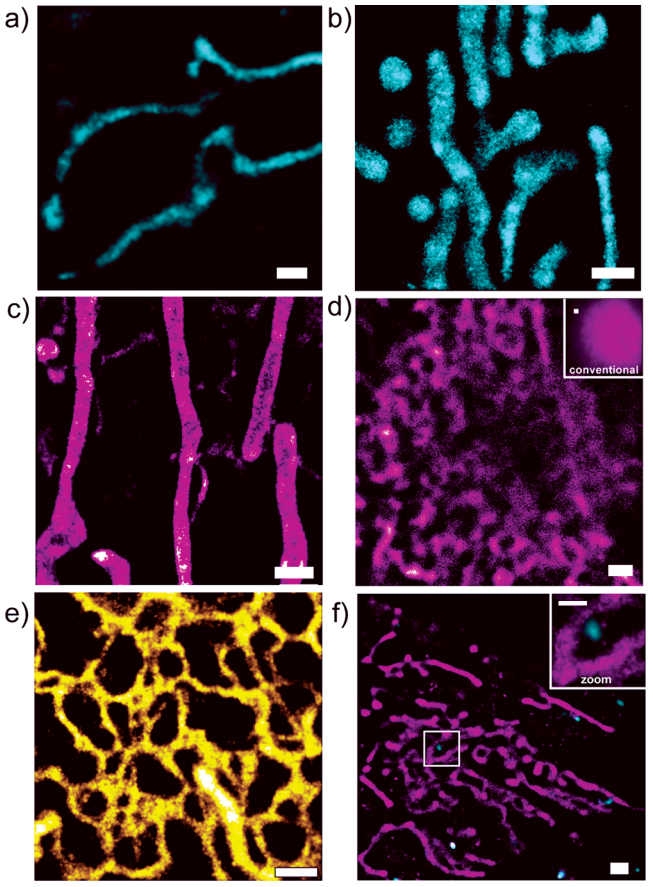

Figure 1. Live SR images of organelles labeled with site-specific stains. Mitochondria stained with (a) JC-9 in Glox + AA, (b) Rhodamine 123 in AA, and (c) TMRE in AA. (d) Dye D staining the Golgi apparatus in Leibovitz. Inset highlights convential image. (e) Nile red labeling the endoplasmic reticulum and mitochondria in Leibovitz. (f) MitoTracker Red CMH_2XRos costained with LysoTracker Green, imaged in Glox + AA. Inset highlights areas where both organelles are present. (a–f) acquisition time: 20 s. Integration times of 2 ms were used to acquire all of the above images. Scale bars: 1 μm.

bright state during a single frame; in such cases, multiemitter algorithms are more appropriate in image reconstruction, as recently shown.[7] The live-cell SR image of the Golgi apparatus (Figure 1d) is a clear improvement over its conventional image (inset Figure 1d), since the membrane folds making up the cisternal stack are now visible. Lastly, Nile red highlights both mitochondria and the ER (Figure 1e). Since these two compartments are morphologically distinct, this stain can provide cellular context by acting as an SR contrast agent in studies of the ER or mitochondria. The sizes of ER tubules and their intersection with mitochondria are readily visible here, providing a clear improvement over the diffraction-limited image (SI Figures 7 e–f and 8e) where the ER tubules are blurred.

To highlight the flexibility of this approach, we performed dual-color SR imaging by staining mitochondria and lysosomes with MitoTracker Red CMH_2XRos and LysoTracker Green, respectively. We selected this combination since both dyes photoswitch under identical buffer conditions (Table 1) and have minimal spectral overlap. Indeed, we found that both dyes blinked well in a mixture of Glox + AA, yielding high-contrast and well-resolved images (Figure 1f). Intriguingly, while imaging these two organelles, we observed the colocalization of mitochondrial staining with a subset of lysosomes; this is evident in the dual-color SR image, where regions of overlap between the red and green channel image are evident. This may indicate mitophagy: the degradation of mitochondria in autolysosomes.[24] Finally, the ease of this mix-and-match choice of labels can be translated to combine site-specific dyes with fluorescent proteins, or with other synthetic dyes targeted using chemical tags.

To quantify dye performance, we considered the temporal resolution achievable with each dye using a procedure recently outlined.[7] Briefly summarizing, the Nyquist criterion, as previously applied to SR[1], dictates that the density of molecules ρ required to resolve features of size R_{min} must be at least $(2/R_{min})^2$ for two-dimensional imaging. Accordingly, we evaluated dyes based on the shortest acquisition time (t_{min}), which fulfils Nyquist with $R_{min} = \sigma$, where σ represents the mean localization precision of single molecules used to construct a given live-cell SR image (see R_{min} *discussion* in Supporting Information and SI Figure 9). For this purpose, we defined regions of interest (ROI) on each structure imaged (Figure 2a), then decreased the number of acquisition frames until the density within the ROI was equal to the limiting Nyquist density (i.e $\rho_{ROI} = (2/\sigma$ nm$)^2$). This acquisition time (Figure 2b) ranges from 6 to 17 s, comparable to previously reported rates for live SR imaging.[1,2,6,7] Once we defined the minimum time required to achieve a suitable molecular density, we made SR movies where each frame is an SR image reconstructed using the Nyquist limiting stack. Over the course of 5 min, we observed the dynamic motion of a mitochondrial junction along with the reshaping of this organelle (Figure 2c). Additionally, over the course of 20 s, we observed the motion of mitochondria ranging from fusion/fission events to small spatial fluctuations (see SI Videos 1, 2, 3). We note that although the Nyquist criteria is commonly used to quantify resolution, and we apply it here to permit direct comparisons with other published work, alternative metrics have also been proposed.[3,25,26] To compare the performance of these dyes with ectopically expressed photoswitchable proteins, we provide estimates of their relative density and brightness (see the *Dyes versus Protein Performance* discussion in the SI).

The data presented here combined with published data on site-specific dyes indicates that there exists a photoswitching dependence on the organelle redox state[14,27,28] and on chromophore structure[29] as previously proposed. We summarize these observations in SI Table 4.

Photoswitching of fluorophores is commonly attributed to transient dark states induced by reducing and oxidizing (ROX) processes.[27] We noticed that some dyes required the addition of an oxygen scavenging system (Glox) and/or a reducing agent (AA) while others were capable of blinking in a live-cell compatible buffer (Leibovitz) alone. This is intriguing, since it supports the idea that some cellular compartments offer certain dyes a nanoenvironment sufficient for photoswitching.[28,30] For instance, we noticed that additives to the imaging media were unnecessary for the BODIPY based ER tracker red targeted to the ER membrane; however, it has been reported that the BODIPY based dye LysoTracker Red photoswitches in lysosomes upon addition of Glox.[7] Because lysosomal membranes have been shown to have similar redox potentials to that of the ER membrane,[31] this suggests that even the small differences in the redox potentials of the ER membrane and lysosomal membrane or differences between the redox potentials of these two red BODIPY dyes could impact their

dx.doi.org/10.1021/cb400467x | *ACS Chem. Biol.* XXXX, XXX, XXX–XXX

a)

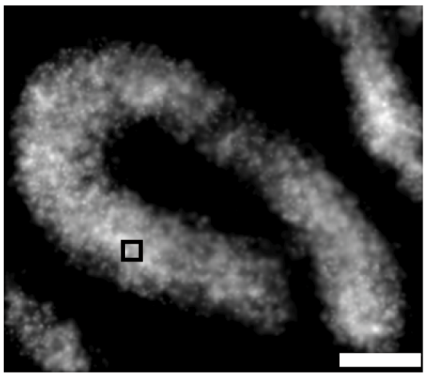

b)

Dye	Imaging medium	Mean localization precision (nm) (± S.D)	Minimum time required to image structure (s) (± S.D)
JC-9	Glox + AA	35 (1)	7 (1)
Rhodamine 123	AA	22 (2)	16 (4)
TMRE	Leib	23 (2)	14 (3)
	AA	23 (1)	11 (2)
	Glox + AA	25 (2)	6 (2)
Dye D	Leib	43 (1)	12 (3)
Nile Red	Leib	30 (2)	17 (2)
	AA	31 (2)	15 (3)
LTG	Glox + AA	26 (1)	14 (1)

c)

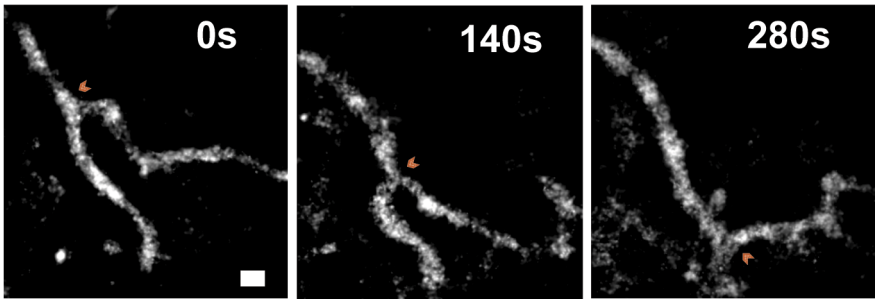

Figure 2. Evaluating dye performance by temporal resolution. (a) The density of molecules is determined within an ROI, shown for mitochondria stained with Rhodamine 123 in AA. (b) The mean localization precision and temporal resolution, t_{min} for the dyes tested. Mean and standard deviation (SD) values were determined from 3 to 5 cells with 5 ROIs per cell. (c) Still frames of a video of TMRE (in AA) staining the mitochondria imaged for 5 min total, where each frame is reconstructed with 11 s of imaging, representing the number of Nyquist limiting frames (t_{min}). From left to right, the stills were imaged at 0, 140, and 280 s after the start of acquisition. Integration times of 2 ms were used to acquire all of the above images and determine temporal resolutions in 2b. The red arrow highlights the junction point to guide the eye. Scale bars: 500 nm.

ability to photoswitch. Another interesting observation related to the compartment dependence of photoswitching can be seen with the red benzophenoxazine dyes Nile red and its derivative Dye D. Specifically, these red dyes were capable of photoswitching in three distinct compartments: mitochondria, the ER membrane, and the Golgi apparatus. Since these compartments have different redox potentials,[31−33] this suggests that benzophenoxazine dyes can photoswitch over a range of intracellular redox states. Thus, it seems that some dye structures such as benzophenoxazine are more amenable than others such as BODIPY to photoswitching under a range of chemical microenvironments.

In addition, it has recently been reported that single-molecule blinking can depend directly on chromophore structure. For cyanine dyes, red-shifted fluorophores have longer off-times than blue-shifted ones due to their larger size; this, in turn yields the more pronounced blinking necessary for SR imaging.[29] Consistent with this, we noticed that dyes of a homologous chromophore series, which were targeted to the same organelle, but varied in color did not have identical photoswitching properties. MitoTracker Green, MitoTracker Red, and MitoTracker Deep Red are all carbocyanine dyes, yet only MitoTracker Deep Red was capable of photoswitching under the tested conditions.[7] Similarly, of the BODIPY-based ER-tracker dyes, the red version proved suitable[7] while the green version did not. Therefore, this trend, which relates chromophore structure, and specifically size, to photoswitching is also observed in two distinct homologous series of site-specific dyes.

We have expanded a labeling strategy based on affinity targeting which does not require the development of orthogonal labeling schemes, since specificity comes from the dyes themselves. We explored the influence of live-cell compatible imaging media on these dyes and evaluated performance in vivo. Their performance was found to be comparable to site-specific dyes previously tested.[7] We expect these dyes to be of great use in live-cell SR studies; in particular, their live-cell compatibility can allow for easy pairing with switchable fluorescent proteins. Identification and screening of more small molecules that specifically label intracellular targets will expand this approach. Experiments were carried out with a limited set of media, but further investigation or the discovery of other noncytotoxic ROX agents could improve imaging. Furthermore, identifying live-cell compatible chemical mechanisms that do not require high laser power for photoswitching will extend the applicability of this approach for live intracellular SR studies.

METHODS

Cell Culture. U2OS cells were maintained in Dulbecco's Modified Eagles's Medium (DMEM) (Gibco) supplemented with 10% Fetal Bovine Serum (FBS) (Gibco) in an atmosphere containing 5% CO_2 at 37 °C. Cells were cultured and maintained in T-25 flasks and grown to about 70% confluency (corresponding to 2 days) before they were passaged. Cells were plated on 25 mm glass coverslips (100 K cells per coverslip) 24 h before imaging was performed.

Cell Staining and Imaging Buffers. Prior to staining, cells were washed once with PBS (Sigma). Dilutions of all dyes were made in Leibovitz (Invitrogen) immediately before labeling cells. Dye concentrations and incubation times varied (see SI Methods for details). All incubations took place at 37 °C in a 5% CO_2 atmosphere.

Following incubation, the cells were washed twice with PBS and imaged in a prewarmed buffer. Experiments were performed in three different buffer conditions: Leibovitz alone, Leibovitz supplemented ascorbic acid (100 μM) (Invitrogen) and Leibovitz with, glucose (10% m/v solution), approximately 0.05% HEPES (pH 7.5, 1M) glucose oxidase (30 μg mL^{-1}) (Invitrogen), catalase (10 μg mL^{-1})

dx.doi.org/10.1021/cb400467x | ACS Chem. Biol. XXXX, XXX, XXX−XXX

(Invitrogen) and ascorbic acid (100 μM) at pH 7.2 (otherwise noted as Glox+AA). To ensure that the Glox buffer did not lead to physiologically unfavorable conditions over the course of imaging experiments, we measured the pH immediately after experiments and found that it did not change.

Live-Cell SR Imaging. Imaging was performed on a custom-built inverted microscope equipped with an oil-immersion objective (Nikon, 100×, NA = 1.49). 488 and 561 nm (TOPTICA photonics) lasers were used. When necessary (for Dye D and LysoTracker Green), a 405 nm laser (OBIS) was used. All lasers were reflected by a 4-color dichroic (89100bs, Chroma). Fluorescence was directed onto an electron multiplying CCD camera (Evolve 128, Photometrics) with a resulting pixel size of 120 nm. For each dye/imaging medium combination, typically 15 000 frames were collected with a 2 ms integration time. For rhodamine 123, LysoTracker Green and JC-9 an ET525/50 (Chroma) emission filter was used; an ET605/70 (Chroma) emission filter was used for MitoTracker Red CMH_2XRos; far red fluorescence corresponding to Nile red was collected after passing through an ET700/75 (Chroma) emission filter. For dual-color experiments, sequential imaging was performed with the MitoTracker Red CMH_2XRos imaged first to prevent photobleaching of the LysoTracker Green. The chromatic shift was corrected using TetraSpek beads (Invitrogen) imaged in the red and green channels. See SI Methods for a description of laser intensity measurements, molecule localization analysis and how SR videos were generated.

■ ASSOCIATED CONTENT

Ⓢ Supporting Information

Additional figures, tables, and methods as described in the text. This material is available free of charge via the Internet at http://pubs.acs.org/.

■ AUTHOR INFORMATION

Corresponding Author

*E-mail: suliana.manley@epfl.ch.

Notes

The authors declare no competing financial interest.

■ ACKNOWLEDGMENTS

We thank H. Hess for the use of Peakselector software, K. Burgess for the golgi Dye D, and P. Schmidt for the XTT reagents. We also thank T. Pengo, N. Olivier, A. Benke, and S. Holden for useful discussions and technical assistance. The research leading to these results has received funding from the European Research Council under the European Community's Seventh Framework Programme/ERC grant agreement number 243016—PALMassembly. The NCCR Chemical Biology, funded by the Swiss National Science Foundation, also supported this research.

■ REFERENCES

(1) Shroff, H., Galbraith, C. G., Galbraith, J. A., and Betzig, E. (2008) Live-cell photoactivated localization microscopy of nanoscale adhesion dynamics. *Nat. Methods 5*, 417−423.

(2) Wombacher, R., Heidbreder, M., van de Linde, S., Sheetz, M. P., Heilemann, M., Cornish, V. W., and Sauer, M. (2010) Live-cell super-resolution imaging with trimethoprim conjugates. *Nat. Methods 7*, 717−719.

(3) Jones, S. A., Shim, S. H., He, J., and Zhuang, X. W. (2011) Fast, three-dimensional super-resolution imaging of live cells. *Nat. Methods 8*, 499−U496.

(4) Benke, A., Olivier, N., Gunzenhauser, J., and Manley, S. (2012) Multicolor single molecule tracking of stochastically active synthetic dyes. *Nano Lett. 12*, 2619−2624.

(5) Shroff, H., Galbraith, C. G., Galbraith, J. A., White, H., Gillette, J., Olenych, S., Davidson, M. W., and Betzig, E. (2007) Dual-color superresolution imaging of genetically expressed probes within individual adhesion complexes. *Proc. Natl. Acad. Sci. U.S.A. 104*, 20308−20313.

(6) Benke, A., and Manley, S. (2012) Live-cell dSTORM of cellular DNA based on direct DNA labeling. *ChemBioChem 13*, 298−301.

(7) Shim, S. H., Xia, C. L., Zhong, G. S., Babcock, H. P., Vaughan, J. C., Huang, B., Wang, X., Xu, C., Bi, G. Q., and Zhuang, X. W. (2012) Super-resolution fluorescence imaging of organelles in live cells with photoswitchable membrane probes. *Proc. Natl. Acad. Sci. U.S.A. 109*, 13978−13983.

(8) van de Linde, S., Sauer, M., and Heilemann, M. (2008) Subdiffraction-resolution fluorescence imaging of proteins in the mitochondrial inner membrane with photoswitchable fluorophores. *J. Struct. Biol. 164*, 250−254.

(9) Bates, M., Huang, B., Dempsey, G. T., and Zhuang, X. W. (2007) Multicolor super-resolution imaging with photo-switchable fluorescent probes. *Science 317*, 1749−1753.

(10) Heilemann, M., van de Linde, S., Schuttpelz, M., Kasper, R., Seefeldt, B., Mukherjee, A., Tinnefeld, P., and Sauer, M. (2008) Subdiffraction-resolution fluorescence imaging with conventional fluorescent probes. *Angew Chem. Int. Ed. 47*, 6172−6176.

(11) Brunelle, J. K., and Chandel, N. S. (2002) Oxygen deprivation induced cell death: An update. *Apoptosis 7*, 475−482.

(12) Chen, H. C., McCaffery, J. M., and Chan, D. C. (2007) Mitochondrial fusion protects against neurodegeneration in the cerebellum. *Cell 130*, 548−562.

(13) Shi, X., Lim, J., and Ha, T. (2010) Acidification of the oxygen scavenging system in single-molecule fluorescence studies: In situ sensing with a ratiometric dual-emission probe. *Anal. Chem. 82*, 6132−6138.

(14) van de Linde, S., Kasper, R., Heilemann, M., and Sauer, M. (2008) Photoswitching microscopy with standard fluorophores. *Appl. Phys. B 93*, 725−731.

(15) Vogelsang, J., Cordes, T., Forthmann, C., Steinhauer, C., and Tinnefeld, P. (2009) Controlling the fluorescence of ordinary oxazine dyes for single-molecule switching and superresolution microscopy. *Proc. Natl. Acad. Sci. U.S.A. 106*, 8107−8112.

(16) van de Linde, S., Loschberger, A., Klein, T., Heidbreder, M., Wolter, S., Heilemann, M., and Sauer, M. (2011) Direct stochastic optical reconstruction microscopy with standard fluorescent probes. *Nat. Protoc. 6*, 991−1009.

(17) Testa, I., Wurm, C. A., Medda, R., Rothermel, E., von Middendorf, C., Folling, J., Jakobs, S., Schonle, A., Hell, S. W., and Eggeling, C. (2010) Multicolor fluorescence nanoscopy in fixed and living cells by exciting conventional fluorophores with a single wavelength. *Biophys. J. 99*, 2686−2694.

(18) Lukinavicius, G., Umezawa, K., Olivier, N., Honigmann, A., Yang, G., Plass, T., Mueller, V., Reymond, L., Correa, I. R., Jr., Luo, Z. G., Schultz, C., Lemke, E. A., Heppenstall, P., Eggeling, C., Manley, S., and Johnsson, K. (2013) A near-infrared fluorophore for live-cell super-resolution microscopy of cellular proteins. *Nat. Chem. 5*, 132−139.

(19) Steinhauer, C., Forthmann, C., Vogelsang, J., and Tinnefeld, P. (2008) Super-resolution microscopy on the basis of engineered dark states. *J. Am. Chem. Soc. 130*, 16840−16841.

(20) Leibovitz, A. (1963) The growth and maintenance of tissue-cell cultures in free gas exchange with the atmosphere. *Am. J. Hyg. 78*, 173−180.

(21) Dempsey, G. T., Vaughan, J. C., Chen, K. H., Bates, M., and Zhuang, X. W. (2011) Evaluation of fluorophores for optimal performance in localization-based super-resolution imaging. *Nat. Methods 8*, 1027.

(22) Lampe, A., Haucke, V., Sigrist, S. J., Heilemann, M., and Schmoranzer, J. (2012) Multi-colour direct STORM with red emitting carbocyanines. *Biol. Cell 104*, 229−237.

(23) Dinant, C., de Jager, M., Essers, J., van Cappellen, W. A., Kanaar, R., Houtsmuller, A. B., and Vermeulen, W. (2007) Activation of multiple DNA repair pathways by sub-nuclear damage induction methods. *J. Cell Sci. 120*, 2731−2740.

(24) Bainton, D. F. (1981) The discovery of lysosomes. *J. Cell Biol. 91*, S66−S76.
(25) Fitzgerald, J. E., Lu, J., and Schnitzer, M. J. (2012) Estimation theoretic measure of resolution for stochastic localization microscopy. *Phys. Rev. Lett. 109*, DOI: 10.1103/PhysRevLett.109.048102.
(26) Nieuwenhuizen, R. P., Lidke, K. A., Bates, M., Puig, D. L., Grunwald, D., Stallinga, S., and Rieger, B. (2013) Measuring image resolution in optical nanoscopy. *Nat. Methods*, 557−562.
(27) Vogelsang, J., Kasper, R., Steinhauer, C., Person, B., Heilemann, M., Sauer, M., and Tinnefeld, P. (2008) A reducing and oxidizing system minimizes photobleaching and blinking of fluorescent dyes. *Angew Chem. Int. Ed. 47*, 5465−5469.
(28) van de Linde, S., Heilemann, M., and Sauer, M. (2012) Live-cell super-resolution imaging with synthetic fluorophores. *Annu. Rev. Phys. Chem. 63*, 519−540.
(29) Stein, I. H., Capone, S., Smit, J. H., Baumann, F., Cordes, T., and Tinnefeld, P. (2012) Linking single-molecule blinking to chromophore structure and redox potentials. *ChemPhysChem 13*, 931−937.
(30) van de Linde, S., Endesfelder, U., Mukherjee, A., Schuttpelz, M., Wiebusch, G., Wolter, S., Heilemann, M., and Sauer, M. (2009) Multicolor photoswitching microscopy for subdiffraction-resolution fluorescence imaging. *Photochem. Photobiol. Sci. 8*, 465−469.
(31) Austin, C. D., Wen, X. H., Gazzard, L., Nelson, C., Scheller, R. H., and Scales, S. J. (2005) Oxidizing potential of endosomes and lysosomes limits intracellular cleavage of disulfide-based antibody-drug conjugates. *Proc. Natl. Acad. Sci. U.S.A. 102*, 17987−17992.
(32) Jones, D. P. (2010) Redox sensing: Orthogonal control in cell cycle and apoptosis signalling. *J. Intern. Med. 268*, 432−448.
(33) Llopis, J., McCaffery, J. M., Miyawaki, A., Farquhar, M. G., and Tsien, R. Y. (1998) Measurement of cytosolic, mitochondrial, and Golgi pH in single living cells with green fluorescent proteins. *Proc. Natl. Acad. Sci. U.S.A. 95*, 6803−6808.
(34) Reers, M., Smith, T. W., and Chen, L. B. (1991) J-aggregate formation of a carbocyanine as a quantitative fluorescent indicator of membrane potential. *Biochemistry 30*, 4480−4486.
(35) Scaduto, R. C., Jr., and Grotyohann, L. W. (1999) Measurement of mitochondrial membrane potential using fluorescent rhodamine derivatives. *Biophys. J. 76*, 469−477.
(36) Jose, J., Loudet, A., Ueno, Y., Barhoumi, R., Burghardt, R. C., and Burgess, K. (2010) Intracellular imaging of organelles with new water-soluble benzophenoxazine dyes. *Org. Biomol. Chem. 8*, 2052−2059.
(37) Kurz, T., Eaton, J. W., and Brunk, U. T. (2010) Redox activity within the lysosomal compartment: Implications for aging and apoptosis. *Antioxid. Redox Signaling 13*, 511−523.